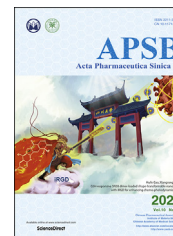




Chinese Pharmaceutical Association  
Institute of Materia Medica, Chinese Academy of Medical Sciences

Acta Pharmaceutica Sinica B

[www.elsevier.com/locate/apsb](http://www.elsevier.com/locate/apsb)  
[www.sciencedirect.com](http://www.sciencedirect.com)



ORIGINAL ARTICLE

# Targeting castration-resistant prostate cancer with a novel ROR $\gamma$ antagonist elaiophylin



Jianwei Zheng<sup>a,†</sup>, Junfeng Wang<sup>b,†</sup>, Qian Wang<sup>a</sup>, Hongye Zou<sup>c</sup>,  
Hong Wang<sup>a</sup>, Zhenhua Zhang<sup>a</sup>, Jianghe Chen<sup>a</sup>, Qianqian Wang<sup>a</sup>,  
Panxia Wang<sup>a</sup>, Yueshan Zhao<sup>a</sup>, Jing Lu<sup>a</sup>, Xiaolei Zhang<sup>a</sup>,  
Songtao Xiang<sup>d</sup>, Haibin Wang<sup>e</sup>, Jinping Lei<sup>a</sup>, Hong-Wu Chen<sup>c</sup>,  
Peiqing Liu<sup>a,f,g</sup>, Yonghong Liu<sup>b,\*</sup>, Fanghai Han<sup>h,\*</sup>, Junjian Wang<sup>a,f,g,\*</sup>

<sup>a</sup>School of Pharmaceutical Sciences, Sun Yat-sen University, Guangzhou 510006, China

<sup>b</sup>CAS Key Laboratory of Tropical Marine Bio-resources and Ecology/Guangdong Key Laboratory of Marine Materia Medica, South China Sea Institute of Oceanology, Chinese Academy of Sciences, Guangzhou 510301, China

<sup>c</sup>Department of Biochemistry and Molecular Medicine, UC Davis Comprehensive Cancer Center, School of Medicine, University of California, Davis, Sacramento, CA 95817, USA

<sup>d</sup>Department of Urology, the Second Affiliated Hospital of Guangzhou University of Chinese Medicine, Guangzhou 510120, China

<sup>e</sup>Department of Joint Orthopaedic, the First Affiliated Hospital, Guangzhou University of Chinese Medicine, Guangzhou 510405, China

<sup>f</sup>National-Local Joint Engineering Laboratory of Druggability and New Drugs Evaluation, Sun Yat-sen University, Guangzhou 510006, China

<sup>g</sup>Guangdong Provincial Key Laboratory of New Drug Design and Evaluation, School of Pharmaceutical Sciences, Sun Yat-sen University, Guangzhou 510006, China

<sup>h</sup>Department of Gastrointestinal Surgery, Sun Yat-sen Memorial Hospital, Sun Yat-sen University, Guangzhou 510120, China

Received 13 March 2020; received in revised form 20 June 2020; accepted 1 July 2020

## KEY WORDS

ROR $\gamma$ ;  
Castration-resistant

**Abstract** Prostate cancer (PCa) patients who progress to metastatic castration-resistant PCa (mCRPC) mostly have poor outcomes due to the lack of effective therapies. Our recent study established the orphan nuclear receptor ROR $\gamma$  as a novel therapeutic target for CRPC. Here, we reveal that elaiophylin (Elai), an

\*Corresponding authors.

E-mail addresses: [yonghongliu@scsio.ac.cn](mailto:yonghongliu@scsio.ac.cn) (Yonghong Liu), [fh\\_han@163.com](mailto:fh_han@163.com) (Fanghai Han), [wangjj87@mail.sysu.edu.cn](mailto:wangjj87@mail.sysu.edu.cn) (Junjian Wang).

<sup>†</sup>These authors made equal contributions to this work.

Peer review under responsibility of Chinese Pharmaceutical Association and Institute of Materia Medica, Chinese Academy of Medical Sciences.

<https://doi.org/10.1016/j.apsb.2020.07.001>

2211-3835 © 2020 Chinese Pharmaceutical Association and Institute of Materia Medica, Chinese Academy of Medical Sciences. Production and hosting by Elsevier B.V. This is an open access article under the CC BY-NC-ND license (<http://creativecommons.org/licenses/by-nc-nd/4.0/>).

prostate cancer;  
Nuclear receptor;  
Antagonist;  
Elaiophylin

antibiotic from *Actinomyces streptomycetes*, is a novel ROR $\gamma$  antagonist and showed potent antitumor activity against CRPC *in vitro* and *in vivo*. We demonstrated that Elai selectively binded to ROR $\gamma$  protein and potently blocked ROR $\gamma$  transcriptional regulation activities. Structure–activity relationship studies showed that Elai occupied the binding pocket with several key interactions. Furthermore, Elai markedly reduced the recruitment of ROR $\gamma$  to its genomic DNA response element (RORE), suppressed the expression of ROR $\gamma$  target genes *AR* and *AR* variants, and significantly inhibited PCa cell growth. Importantly, Elai strongly suppressed tumor growth in both cell line based and patient-derived PCa xenograft models. Taken together, these results suggest that Elai is novel therapeutic ROR $\gamma$  inhibitor that can be used as a drug candidate for the treatment of human CRPC.

© 2020 Chinese Pharmaceutical Association and Institute of Materia Medica, Chinese Academy of Medical Sciences. Production and hosting by Elsevier B.V. This is an open access article under the CC BY-NC-ND license (<http://creativecommons.org/licenses/by-nc-nd/4.0/>).

## 1. Introduction

Metastatic castration-resistant prostate cancer (mCRPC) remains one of the leading causes of cancer-related death in men<sup>1</sup>. Next-generation anti-androgen therapeutics enzalutamide (ENZ) and abiraterone (ABI) are being used as one of the standard first-line therapies for the treatment of mCRPC and showing improvement of the disease outcomes in some patients. However, most tumors develop resistance and advance to incurable diseases<sup>2,3</sup>. One major mechanism of ABI or ENZ resistance is that tumor cells up-regulate the expression of androgen receptor (AR) variants (ARVs)<sup>4–7</sup>. Unlike AR full-length (AR-FL), most of the variants lack functional ligand binding domain (LBD) and thus are not responsive to anti-androgen therapies<sup>7</sup>, which limits the significance of developing more potent anti-androgens. Therefore, new therapeutic strategies for metastatic castration-resistant PCa (mCRPC) are urgently needed.

The RAR-related orphan receptors (RORs) are members of the nuclear receptor superfamily and consist of ROR $\alpha$ ,  $\beta$ , and  $\gamma$ <sup>8,9</sup>. They control gene expression by directly binding to their corresponding genomic sites, and have different physiological functions. T cells have a specific ROR $\gamma$  isoform, namely ROR $\gamma$ t, which differs in the N-terminal, less than 20 amino acids, due to T cell-specific promoter usage<sup>7</sup>. It is well established that ROR $\gamma$ t plays a crucial role in inflammation-associated Th17 cell development and autoimmune diseases<sup>10</sup>. Intensive studies are focused on therapeutic development targeting it in autoimmune diseases<sup>8,11–13</sup>. However, the roles of ROR $\gamma$  in human diseases remain largely unclear. Recently, works from our group and others established that ROR $\gamma$  is potential therapeutic target for the treatment of cancers<sup>14–16</sup>. In CRPC tumors, ROR $\gamma$  is overexpressed and/or amplified, and functions as a key determinant of AR overexpression and aberrant signaling. The inhibition of ROR $\gamma$  strongly suppresses AR-FL and ARVs expression, and potently blocks CRPC cell growth *in vivo* and *in vitro*<sup>14</sup>. Thus, targeting ROR- $\gamma$  is a promising strategy for effective CRPC therapy and overcoming anti-androgen therapeutic resistance.

Natural products have been a major source of drugs for the treatment of various diseases for thousands of years<sup>17,18</sup>. More than 40% of antitumor drugs are developed from natural sources<sup>19</sup>. Compared with natural products from terrestrial life, discovery and utilization of marine natural products for drug development are uncommon. At present, only a handful of drugs from marine sources have been approved by U.S. Food and Drug Administration (FDA) or the European Medicines Agency (EMA)

and used in clinical treatment of diseases such as cancers<sup>20</sup>. Marine natural products have a high diversity of chemical structures, which are considered to be the most promising and sustainable medicine source. With the advancement of technology, the number of identified marine natural products has increased dramatically<sup>21</sup>.

In this study, we demonstrated that elaiophylin (Elai), an antibiotic obtained from marine-derived *Actinomyces streptomycetes* sp. SCSIO 41398<sup>22</sup>, is a novel ROR $\gamma$  inhibitor and possesses a potent anti-tumor activity against CRPC *in vitro* and *in vivo* through suppressing the expression of AR-FL and ARVs. Our results suggest that Elai might be a drug candidate for the treatment of human CRPC.

## 2. Materials and methods

### 2.1. Cell culture and chemicals

22Rv1 and VCaP were from American Type Culture Collection (ATCC, Manassas, VA, USA). C4-2B was from UroCor Inc. (Oklahoma City, OK, USA). C4-2B and 22Rv1 cells were cultured in RPMI1640 medium, VCaP and 293T cells were cultured in Dulbecco's modified Eagle's medium (DMEM). All culture media were supplemented with 10% fetal bovine serum and 1  $\times$  penicillin/streptomycin (Gibco, Grand Island, NY, USA). Cells were cultured at 37 °C in a humidified incubator containing 5% CO<sub>2</sub>. Elaiophylin (Elai) was purchased from APEXBIO (Houston, TX, USA) and ACMEC (Shanghai, China). Other chemicals were purchased from Sigma–Aldrich (St. Louis, MO, USA) unless specified otherwise.

### 2.2. Cell viability

Cells were seeded in 96-well plates at 500–1000 cells per well (optimum density for growth) in a total volume of 100  $\mu$ L of media. Serially diluted compounds in 250  $\mu$ L of media were added 50  $\mu$ L to the cells per well 24 h later. After 4 days of incubation, Cell-Titer GLO reagents (Promega Corp., Madison, WI, USA) were added, and luminescence was measured on GLOMAX microplate luminometer (Promega Corp.) according to the manufacturer's instructions. The results were presented as percentages and vehicle-treated cells set at 100.

### 2.3. Colony formation

Colony formation was performed as described previously<sup>23</sup>, 500 cells were seeded in each well of 6-well plates and cultured for 12–14 days with the medium changed as well as the compound added every 3 days. Cells were then fixed in 4% paraformaldehyde for 15 min. The plates were washed with PBS three times. Cell colonies were stained with crystal violet for 15 min. The numbers of colonies were counted after being washed three times with PBS.

### 2.4. Caspase-3/7 activity and cell growth

For apoptosis, caspase-3/7 activity was measured as in a previous report<sup>16</sup>. Briefly, caspase-3/7 activity was measured by using a luminescent caspase-Glo 3/7 assay kit (Promega Corp.) following the manufacturer's instructions. Cell protein concentration was quantified to normalize the results. For cell growth, cells were seeded in 6-well plates at  $1.5 \times 10^5$  per well and treated as indicated. Total viable cell numbers were counted by a Coulter cell counter.

### 2.5. Surface plasmon resonance (SPR) analysis

SPR measurements were performed on a Biacore 8K instrument (GE Healthcare, Piscataway, NJ, USA). Briefly, purified ROR $\gamma$  and ROR $\alpha$  (200  $\mu$ g/mL, pH 8.0) were immobilized ( $\sim 10,000$  RU) on a Series S Sensor Chip (GE Healthcare, Piscataway, NJ, USA) according to a standard amine coupling procedure. PBS (G0002, pH 7.2–7.4; Servicebio, Wuhan, China) with 5% DMSO, was used as the running buffer for immobilization. After immobilization, the solution of Elai was prepared with running buffer through serial dilutions of stock solution. Nine concentrations of Elai were injected simultaneously at a flow rate of 65  $\mu$ L/min for 60 s of association phase at 25  $^{\circ}$ C. The final graphs were obtained by subtracting blank sensorgrams. Experimental data were collected with the Biacore 8K manager software and were analyzed to fit to an appropriate binding model to obtain the equilibrium dissociation constant ( $K_d$ ).

### 2.6. Transient transfection and luciferase assays

Transient transfections were performed using Lipofectamine 2000 (Invitrogen, Carlsbad, CA, USA). For luciferase reporter gene assays, 293T cells were seeded at  $10^4$  cells per well in 96-well plates in phenol red-free DMEM medium (Hyclone, Logan, UT, USA) supplemented with 10% (*v/v*) charcoal stripped fetal bovine serum and co-transfected with pBD-ROR $\gamma$ -LBD (25 ng per well) and pFR-luci (25 ng per well), with pcDNA-PGC-1 $\alpha$  (10 ng per well) plasmids or PLX304-V5(N)-ROR $\gamma$  (25 ng per well) and pGL3-AR-ROR $\gamma$  (25 ng per well) plasmids. Renilla luciferase plasmid (40 ng per well) was used as an internal control. Twenty-four hours after transfection, transfected cells were treated with Elai for another 24 h before cells were harvested for luciferase assays. Luciferase activity was performed following the Dual-Luciferase Reporter Assay System introduction (Promega Corp.).

### 2.7. Chromatin immunoprecipitation (ChIP) assay

ChIP assay was performed as our previous work<sup>14</sup>. C4-2B cells were treated with vehicle or Elai (1  $\mu$ mol/L) for 24 h before harvested for ChIP analysis. Anti-ROR $\gamma$  rabbit serum was

described previously<sup>14</sup>. The primers are shown in Supporting Information Table S1.

### 2.8. qRT-PCR

Total RNA was extracted from cells in 6-well plates. cDNA was prepared according to the manufacturer's protocol. PCR was performed on a BIO-RAD CFX96<sup>TM</sup> (BIO-RAD, San Diego, CA, USA) in the presence of SYBR Green. After the fluorescence values were collected, a melting-curve analysis was performed. The experiments were performed at least three times, with data presented as mean  $\pm$  standard deviation (SD). The sequences of primers for the qRT-PCR analysis are listed in Supporting Information Table S2.

### 2.9. Western blotting

Western blotting was performed as in our previous work<sup>23,24</sup>. Antibodies specifically against ROR $\gamma$ , AR, and the other related proteins were used. All the antibodies used in this study are described in the Supporting Information Table S3.

### 2.10. Molecular docking

The crystal structure of ROR $\gamma$  in complex with the antagonist XY101 (PDB code: 4J1L.pdb) was downloaded from Protein Data Bank (<http://www.pdb.org>). The antagonist XY101 was removed from the protein structure, the hydrogen atoms and disulfide bonds of the protein were added by AmerTools. To obtain a large binding pocket for the two compounds Elai and halichoblelide D (Hali), we first performed a 100-ns classical molecular dynamic (MD) simulation for the protein following the same protocol as in our previous studies<sup>25,26</sup> by using the AMBER12 package<sup>27</sup>. Then we chose the snapshot from the 40-ns MD simulation for the subsequent molecular docking modeling. The molecular docking was performed by Schrödinger program following our previous study<sup>28</sup>. The ligand and protein parameters for docking were prepared by Maestro (version 10.1, Schrödinger, LLC, New York, NY, 2015). The Glide docking program in Maestro 10.1 was used for docking studies. For Glide docking, the grid was defined using a 30  $\text{Å}$  box centered on residue MET365 of ROR $\gamma$ , and the important water molecules around the ligand were kept. All parameters were kept as default. The designed molecules were docked using Glide XP mode, and the predicted binding modes of both Elai and Hali were ranked according to their glide scores.

### 2.11. Animal experiments

Four-week-old male NOD/SCID mice (body weight  $\sim 18$  g) were purchased from Nanjing Biomedical Research Institute of Nanjing University (Nanjing, China). Briefly,  $1 \times 10^7$  22Rv1 cells were suspended in total of 100  $\mu$ L PBS and matrigel (1:1), and implanted subcutaneously into the dorsal flank of the mice. When the tumor volume was reached about 50 mm<sup>3</sup>, the mice were grouped randomly. Then mice were divided into two groups ( $n > 6$ ) randomly and treated intraperitoneally (i.p.) with 100  $\mu$ L of either vehicle or Elai (2 mg/kg) for five times per week. Tumor volume and body weight were measured two times per week. The volume was calculated with Eq. (1):

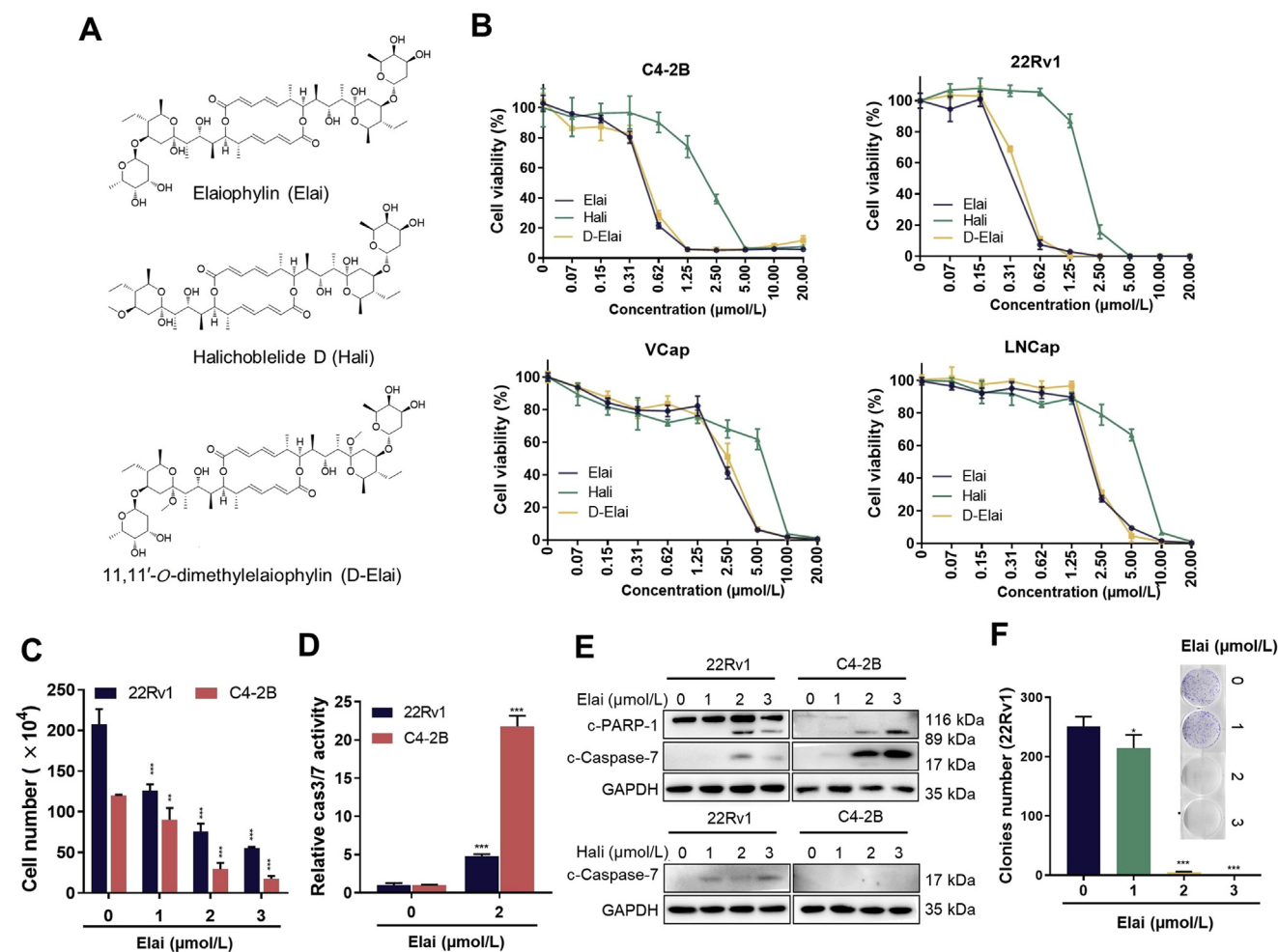


**Figure 1** Elai inhibits castration-resistant prostate cancer cell survival and induces their apoptosis. (A) Chemical structures of elaiophyllin (Elai), halichoblelide D (Hali) and 11,11'-O-dimethylelaiophyllin (D-Elai). (B) Cell viability were measured by Cell-Titer GLO (Promega) of C4-2B, 22Rv1, VCap and LNCaP cells treated with the indicated concentrations of Elai, Hali and D-Elai for 4 days. Experiments were performed three independent times and sextuplicate. (C) 22Rv1 cells and C4-2B cells were treated with vehicle or Elai as indicated. After 24 h, total viable cells were counted with a Coulter cell counter. (D) 22Rv1 and C4-2B cells were treated with vehicle or Elai for 24 h before collected for apoptosis analysis by measuring caspase-3/7 (Cas3/7) activities. (E) Immunoblotting analysis of the indicated proteins in 22Rv1 and C4-2B cells treated with vehicle or Elai or Hali for 24 h. (F) 22Rv1 cells were treated with vehicle (DMSO) or the indicated concentrations of Elai for 12 days, after which colony formation was assessed. All data shown above are mean  $\pm$  SD of three independent experiments. \* $P < 0.05$ , \*\* $P < 0.01$ , \*\*\* $P < 0.001$  vs. control.

$$V = \pi/6 (\text{Length} \times \text{Width}^2) \quad (1)$$

The mice were sacrificed at the end of the studies. Tumors were harvested, weighted and analyzed by immunohistochemistry and immunoblotting assays as previous report<sup>14</sup>. The patient-derived xenograft (PDX) tumor model, PDX-TM00298, was purchased from the Jackson laboratory. The PDX tumors were propagated in the dorsal flank on both sides of the mice. The effect of Elai on PDX tumor growth was evaluated as above description. All animal care and experiments were approved by the Institutional Animal Care and Use Committee of Sun Yat-sen University (Guangzhou, China).

### 2.12. Statistical analysis

All analyses were conducted with GraphPad Prism7 (GraphPad Software, USA). The data are presented as mean  $\pm$  SD from three

independent experiments. Statistics analysis was performed using two-tailed Student's *t*-tests to compare the means.  $P < 0.05$  was considered to be significant.

## 3. Results

### 3.1. Elai inhibits castration-resistant prostate cancer (CRPC) cell survival and induces their apoptosis

To search for drug candidates for the treatment of human CRPC, we screened a chemical library, which contains 500 marine natural compounds, for their activities in growth inhibition of a CRPC cell line C4-2B. Elaiophyllin (Elai) and its derivative 11,11'-O-dimethylelaiophyllin (D-Elai) exhibited a strong activity in inhibition of C4-2B cell survival, while halichoblelide D (Hali) showed less potent inhibition (Fig. 1A and B). Moreover, strong growth inhibition by Elai was observed in other prostate cancer cell lines

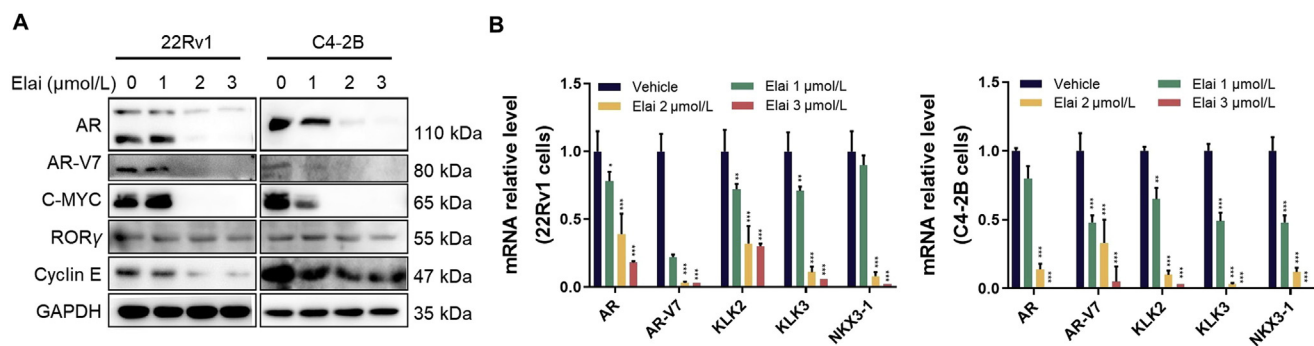


**Figure 2** Elai inhibits AR expression and signaling. (A) Immunoblotting analysis of the indicated proteins in 22Rv1 and C4-2B cells treated with vehicle or Elai for 24 h. (B) qRT-PCR analysis of the indicated genes in 22Rv1 and C4-2B cells treated with vehicle or Elai for 24 h. All data shown above are mean  $\pm$  SD of three independent experiments. \* $P < 0.05$ , \*\* $P < 0.01$ , \*\*\* $P < 0.001$  vs. control.

22Rv1, VCaP and LNCaP cells at nanomolar concentration (Fig. 1B and C). We also found that Elai could strongly induce apoptosis of 22Rv1 and C4-2B cells, as demonstrated by measuring caspase-3/7 (Cas3/7) activities (Fig. 1D). Also, the expression of apoptosis-related proteins such as cleaved-PARP-1 and cleaved-caspase 7 were increased after treatment with Elai (Fig. 1E). Consistent with the effects of Elai on CRPC cell growth and apoptosis, Elai potently reduced CRPC cellular colony formation (Fig. 1F and Supporting Information Fig. S1). These data suggest that Elai inhibits CRPC cell survival and induce their apoptosis *in vitro*.

### 3.2. Elai inhibits the expression of AR-FL and AR-V7 and AR-mediated signaling

Since androgen receptor (AR) and its variants are highly over-expressed in the majority of CRPC tumors and play a pivotal role in the PCa development and progression, we thus examined whether Elai inhibited CRPC cell survival *via* blocking AR signaling. Indeed, we observed that Elai significantly inhibited the expression of AR and its variants at both mRNA and protein level in a dose-dependent manner (Fig. 2A and B). Moreover, Elai decreased the expression of proliferation and survival proteins

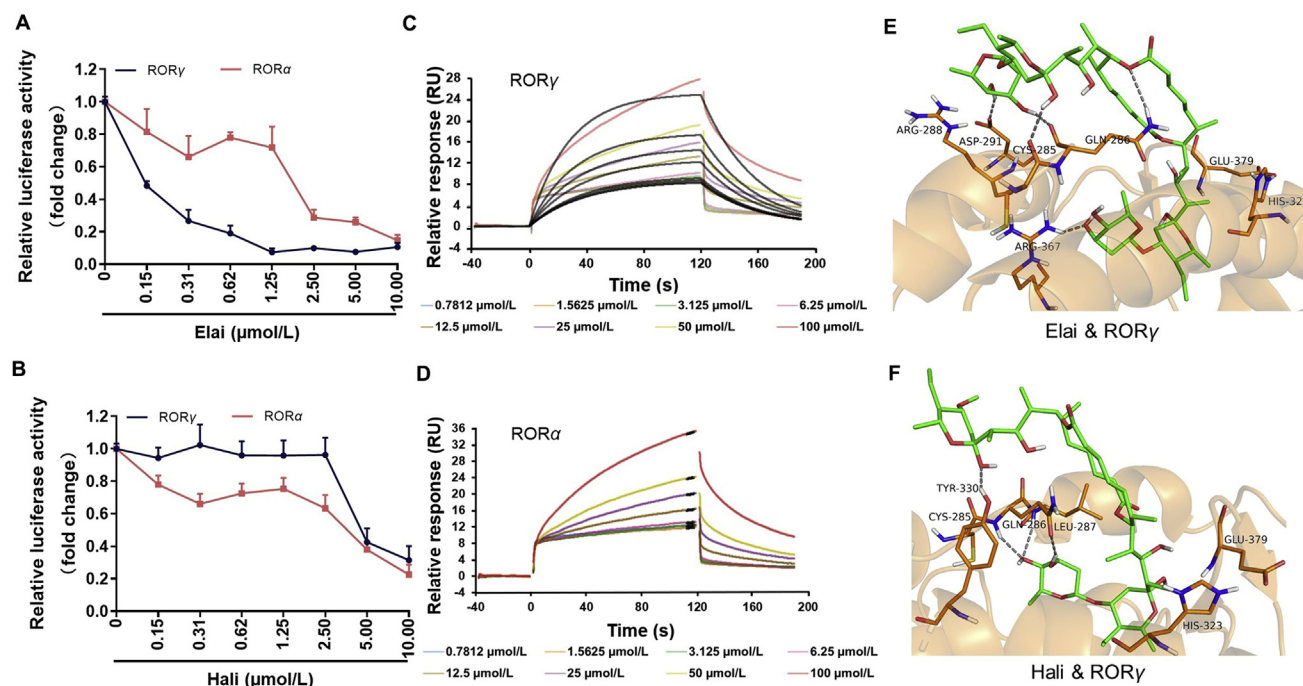


**Figure 3** Identification of Elai as a novel ROR $\gamma$  antagonist. ROR $\gamma$  and ROR $\alpha$  LBD guide-gene reporter assays, with 293T cells showing the effects of Elai (A) and Hali (B) on ROR $\gamma$  and ROR $\alpha$  activation. Fold change indicates the activities of ROR $\gamma$  and ROR $\alpha$  under influence of Elai compared to control set as 1. The data are mean  $\pm$  SD,  $n = 3$ . SPR analysis of the binding affinity of Elai to ROR $\gamma$  (C) and ROR $\alpha$  (D) protein. Apparent equilibrium dissociation constants ( $K_d$ ) were then calculated as the ratio of  $k_d/k_a$ . The  $K_d$  (mol/L) value between Elai and ROR $\gamma$  is  $5.05 \times 10^{-6}$ , while the value for Elai and ROR $\alpha$  is  $2.62 \times 10^{-5}$ . 3D presentation of the predicted binding mode of Elai (E) and Hali (F) with ROR $\gamma$  by molecular docking. The hydrogen bonds were labeled by dashed lines.

such as MYC and cyclin E. Further examination by qRT-PCR analysis showed that Elai strongly suppressed the expression of AR target genes *KLK3*, *KLK2* and *NKX3-1* (Fig. 2B). Therefore, these data suggest that Elai inhibits AR signaling pathway by suppressing the expression of AR gene.

### 3.3. Identification of Elai as a novel ROR $\gamma$ antagonist

Our previous study demonstrated that ROR $\gamma$  is a key determinant of AR gene expression<sup>14</sup>. This promoted us to examine whether Elai suppressed AR gene expression *via* inhibition of ROR $\gamma$  activity in CRPC cells. Using cell-based luciferase reporter assays, we found that Elai strongly suppressed ROR $\gamma$  activity while Hali was less potent (Fig. 3A and B), which is consistent with effects of compounds on CRPC cell survival. Moreover, Elai showed only moderate inhibition on ROR $\alpha$  activities (Fig. 3A). Next, we performed surface plasmon resonance (SPR) assays to determine whether Elai would directly bind to the LBDs of RORs, and found that Elai had a high affinity to the ROR $\gamma$  protein ( $K_d = 5.05 \times 10^{-6}$  mol/L) than ROR $\alpha$  ( $K_d = 5.05 \times 10^{-5}$  mol/L, Fig. 3C and D).

We then performed molecular docking to predict the binding mode and investigate the Elai–ROR $\gamma$  interaction details. Molecular docking as illustrated in Fig. 3E and F demonstrates that both Elai and Hali bound to the ROR $\gamma$  binding pocket as general antagonists<sup>28</sup> through several hydrogen bonds. For Elai, the tetrahydropyranol group inserted into the binding pocket only forms H-bond with ARG367, while the tetrahydropyranol group exposed in the solvent forms H-bonds with ASP291, CYS285 and GLN286. In addition, the exposed carboxylate oxygen atom in the big ring of Elai forms H-bond with GLN286. Whereas, for Hali, the inserted tetrahydropyranol group forms H-bonds with ASP291, CYS285 and GLN286, while the exposed group only forms H-bond with TYR330. Moreover, Elai inserted much deeper into the binding pocket than Hali, and the exposed groups of Elai bind tighter than those of Hali. In addition, the Glide XP score for the binding mode of Elai is higher than Hali (–9.44 vs.

–8.57 kcal/mol). These binding affinities were in line with the above inhibition of Elai and Hali D on ROR $\gamma$  activities. Taken together, our results suggest that Elai is a novel, selective and potent ROR $\gamma$  antagonist.

### 3.4. Elai inhibits AR gene expression and cell survival *via* suppressing ROR $\gamma$ activity

Our previous study demonstrated that ROR $\gamma$  could directly bind to an AR-RORE site in the first exon of AR gene to drive its expression<sup>14</sup>. Moreover, our ROR $\gamma$  ChIP-seq analysis also showed apparent ROR $\gamma$  occupancy peak at the AR-RORE site<sup>16</sup>. We thus performed ChIP-qPCR analysis and found that Elai strongly reduced ROR $\gamma$  binding to AR-RORE site (Fig. 4A). In addition, using a cellular AR-RORE driven gene report assay, we found that Elai significantly suppressed ROR $\gamma$  transcriptional activity in a dose dependent manner (Fig. 4B). To provide further evidence that Elai reduced cell viability *via* inhibiting ROR $\gamma$  activity, we used *RORC* siRNA approach to specifically silence ROR $\gamma$  and demonstrated that Elai-induced inhibition of cell survival was significantly attenuated in *RORC* siRNA treated cells compared to control cells (Fig. 4C). Moreover, ROR $\gamma$  silencing also blocked the inhibition of Elai on prostate cancer cell colony formation (Supporting Information Fig. S2). These data collectively suggest that Elai inhibits AR gene expression and cell survival *via* suppressing ROR $\gamma$  activity.

### 3.5. Elai inhibits CRPC cell autophagy *via* suppressing ROR $\gamma$ activity

It has been reported that Elai inhibited autophagic flux *via* increasing the amount of SQSTM1<sup>29</sup>, meanwhile, our previous gene profiling study also revealed that inhibition of ROR $\gamma$  with selective antagonist SR2211 and XY011 strongly increased the expression of SQSTM1 in CRPC cells<sup>14</sup>. This promoted us to examine whether ROR $\gamma$  was involved in Elai induced inhibition of autophagic flux in CRPC cells. Firstly, we performed

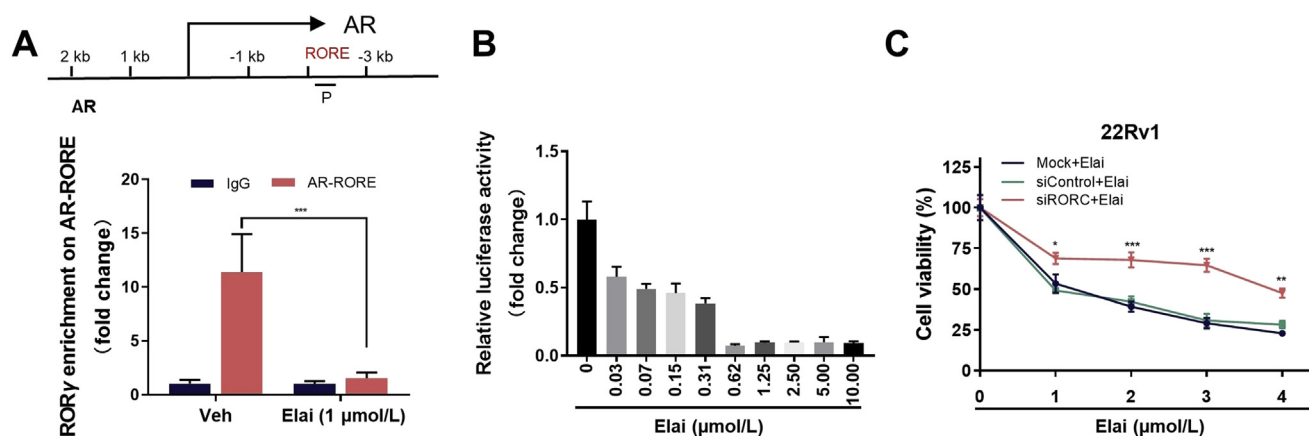


**Figure 4** Elai inhibits AR gene expression and cell survival *via* suppressing ROR $\gamma$  activity. (A) ChIP-qPCR analysis of relative enrichment of ROR $\gamma$  at AR-RORE site of AR gene in C4-2B cells treated with vehicle or Elai for 24 h. Fold change means the indicated enrichment on AR-RORE under influence of Elai compared to the IgG enrichment in cells treated with vehicle control set as 1. (B) AR-RORE driven gene report assay with 293T cells showing the effects of Elai on ROR $\gamma$  transcriptional activity. Fold change indicates the activities of ROR $\gamma$  under influence of Elai compared to control set as 1. (C) 22Rv1 cells were transfected with *RORC* or control siRNA for 48 h and treated with vehicle or Elai for another 24 h. Cells were harvested for determining cell growth by counting viable cells. All data shown above are mean  $\pm$  SD of three independent experiments. \* $P < 0.05$ , \*\* $P < 0.01$ , \*\*\* $P < 0.001$  vs. control.

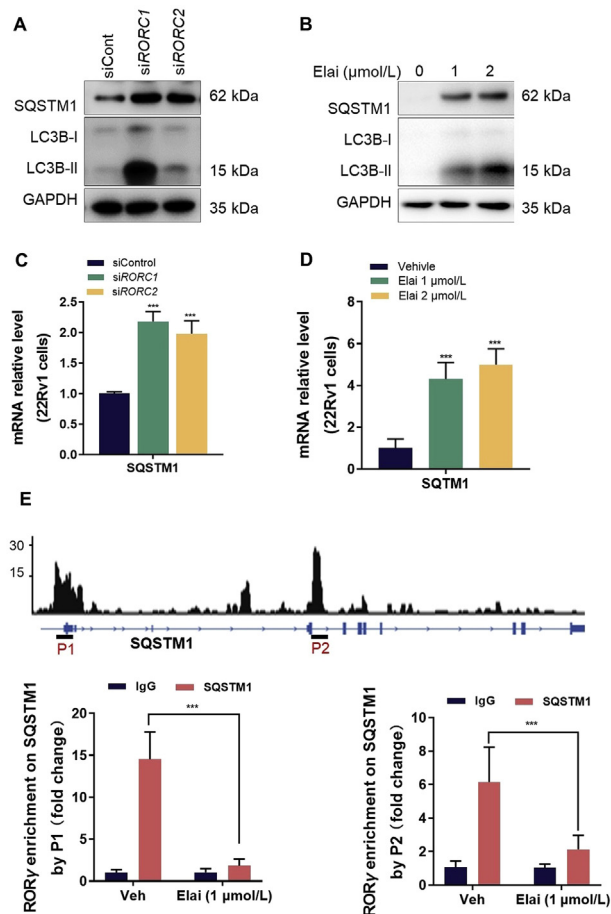


**Figure 5** Elai inhibits CRPC cell autophagy *via* suppressing ROR $\gamma$  activity. (A) 22Rv1 cells were transfected with control or *RORC* siRNA and cultured for 3 days before collected for immunoblotting with specific antibodies against indicated proteins. (B) Immunoblotting analysis of the indicated proteins in 22Rv1 cells treated with vehicle or Elai for 24 h. (C) 22Rv1 cells were transfected with control or *RORC* siRNA and cultured for 2 days before collected for qRT-PCR analysis of the indicated genes. (D) qRT-PCR analysis of the indicated genes in 22Rv1 cells treated with vehicle or Elai for 24 h. (E) Genome browser display of ROR $\gamma$ -binding events on promoter and body of *SQSTM1* gene, data from our previous ChIP-seq data (GSE126380) (upper) ChIP-qPCR analysis of relative enrichment of ROR $\gamma$  at *SQSTM1* gene promoter in C4-2B cells treated with vehicle or Elai for 24 h (bottom). Fold change means the indicated enrichment on *SQSTM1* gene under influence of Elai compared to the IgG enrichment in cells treated with vehicle control set as 1. All data shown above are mean  $\pm$  SD of three independent experiments. \* $P < 0.05$ , \*\* $P < 0.01$ , \*\*\* $P < 0.001$  vs. vehicle control.

immunoblotting for LC3B to validate the effects of ROR $\gamma$  knockdown and Elai on autophagy. Our results show that silencing ROR $\gamma$  with specific *RORC* siRNA significantly increased LC3B-II accumulation in CRPC cells. Interestingly, Elai treatment resulted in a similar increase of LC3B-II expression (Fig. 5A and B). Moreover, both Elai and ROR $\gamma$  knockdown significantly increased the expression of SQSTM1 at both mRNA and protein level (Fig. 5A–D). Since our previous ChIP-seq data showed that the promoter and enhancer regions of *SQSTM1* gene were occupied by ROR $\gamma$  protein<sup>16</sup> (Fig. 5E, upper panel), we performed ChIP-qPCR analysis to determine whether Elai treatment affects ROR $\gamma$  binding to the *SQSTM1* gene regulatory sites and found that Elai strongly reduced ROR $\gamma$  occupancy on the *SQSTM1* promoter (P1) and enhancer (P2) sites (Fig. 5E). Taken together, these data demonstrated that Elai might inhibit CRPC cell autophagy *via* increasing ROR $\gamma$  mediated *SQSTM1* gene expression.

### 3.6. Elai inhibits CRPC tumor growth *in vivo*

We next assessed the effects of Elai on prostate cancer tumor growth. Elai (2 mg/kg, five times per week) or vehicle was intraperitoneally injected into mice bearing 22Rv1 xenograft tumors. Tumor volume and body weight were monitored twice a week. Results showed that Elai strongly suppressed tumor growth compared with vehicle group, and did not cause any significant change in mice body weight (Fig. 6A–C). Immunohistochemical Ki67 staining of the tumor sections showed that Elai significantly inhibited cancer cell proliferation (Fig. 6D). Meanwhile, immunoblotting analysis of xenograft tumors demonstrated that Elai significantly decreased the expression of AR and AR-V7, and increased the level of cleaved-caspase 7 and cleaved-PARP-1 which indicated induction of apoptosis (Fig. 6E). We also investigated the effect of Elai on autophagy in the xenograft tumors and found that Elai inhibited autophagy significantly with the

accumulation of LC3B-II (Supporting Information Figs. S3A and S3B), which indicated that the inhibition of autophagy might play a role in Elai blocking CRPC tumor growth. Moreover, we examined the effect of Elai on a patient derived prostate cancer xenograft model (PDX), results also showed that Elai significantly suppressed the tumor growth of this PDX model (Fig. 6F and G). These results demonstrated that Elai might be a drug candidate for prostate cancer therapy.

#### 4. Discussion

Although significant progress has been made in the field of anti-androgen therapies for CRPC, *de novo* and acquired resistance to these therapies appear inevitable<sup>30</sup>. Development of novel therapeutic agents based on new targets may be able to overcome current CRPC resistance. Our recent study identified ROR $\gamma$  as a novel therapeutic target for CRPC<sup>14</sup>. Here, we demonstrated that

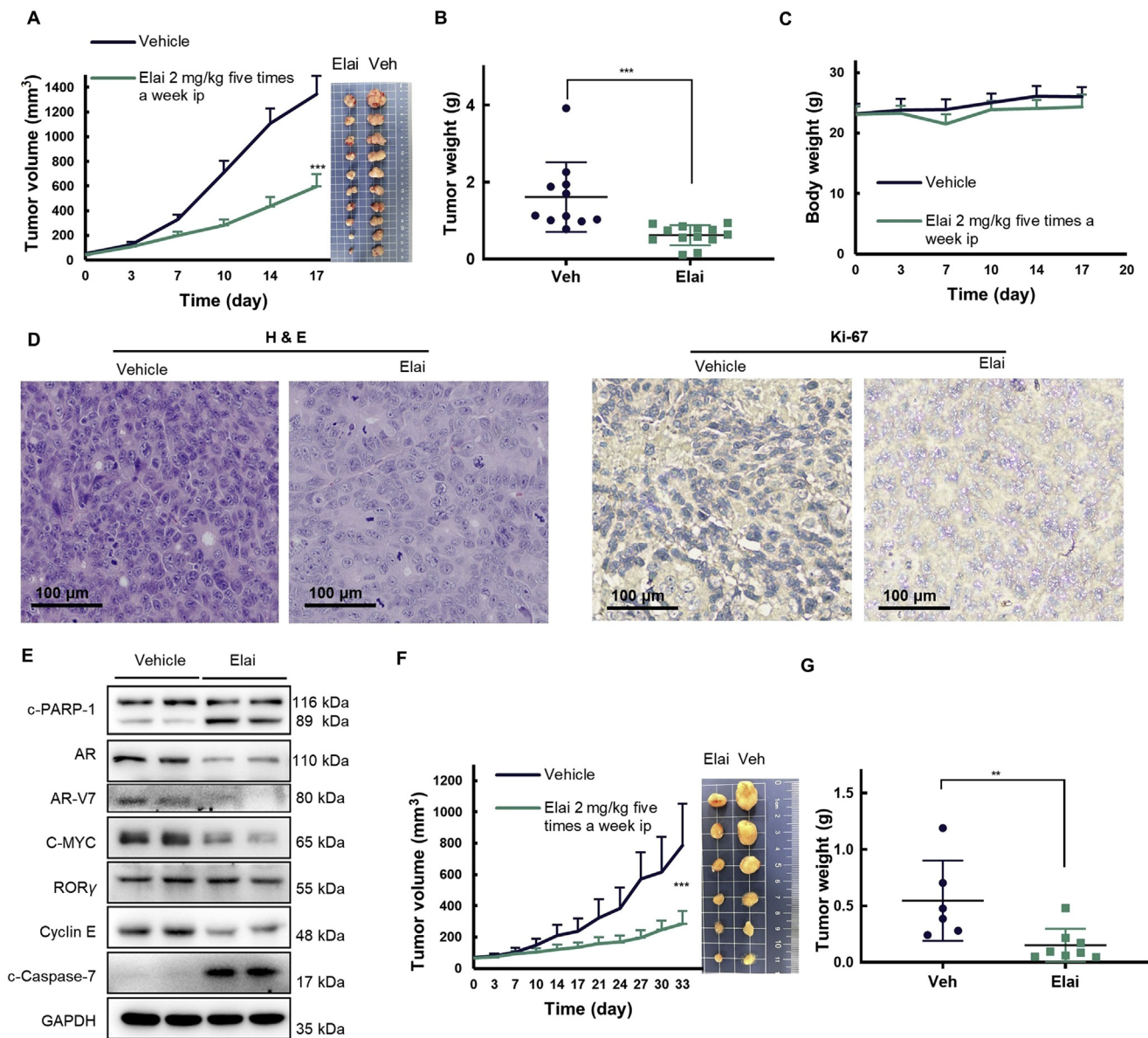


**Figure 6** Elai inhibits CRPC tumor growth *in vivo*. SCID mice bearing 22Rv1 xenografts received Elai (intraperitoneally i.p., 2 mg/kg) or vehicle for five times per week. Mean tumor volume $\pm$ standard error of mean (SEM) (A), mean tumor weight $\pm$ SEM (B), mean body weight $\pm$ SEM (C) and representative tumor images (A) are shown. \*\*\* $P < 0.001$  vs. vehicle control. (D) Anti-Ki67 immunohistochemistry images and H&E staining of tumor section were shown. (E) Immunoblotting analysis of 22Rv1 xenograft tumors after 17 days of treatment with vehicle or Elai as in (A). SCID mice bearing prostate cancer patient derived xenografts (PDX) received Elai (intraperitoneally i.p., 2 mg/kg) or vehicle for five times per week. Mean tumor volume $\pm$ SEM (F), mean tumor weight $\pm$ SEM (G) and representative tumor images (F) are shown. \*\* $P < 0.01$  vs. vehicle control.

Elai is a novel ROR $\gamma$  antagonist and that it showed potent anti-tumor activity against CRPC *in vitro* and *in vivo*.

Since AR plays crucial roles in the vast majority of PCA development and progression<sup>31–34</sup>, current therapeutic development for CRPC still targets the androgen–AR axis *via* suppressing androgen production or blocking AR activation. However, high potent agents targeting the steps after AR gene being overexpressed cannot overcome AR variants induced therapeutic resistance. Our previous report has revealed that ROR $\gamma$  inhibition effectively blocked CRPC tumor growth *via* directly suppressing the expression of AR and its variants<sup>23</sup>. Here, we identified Elai as a novel ROR $\gamma$  antagonist. SPR analysis and gene report assays demonstrated that Elai selectively bound to ROR $\gamma$  protein and potently blocked ROR $\gamma$  activation. In CRPC cells, Elai markedly suppressed the expression of ROR $\gamma$  target genes *AR/AR* variants and significantly inhibited PCa cell growth *via* suppressing ROR $\gamma$  activity. Moreover, employing both cell line-derived based and patient-derived PCa xenograft models, we further demonstrated that Elai strongly suppressed PCa tumor growth *in vivo*.

Our gene expression profiling data showed that the impact of ROR $\gamma$  inhibition on tumor growth was unlikely to be limited to suppressing AR and its programs<sup>14,16</sup>. In addition to reducing AR levels, ROR $\gamma$  inhibition also increased the expression of autophagy adaptor SQSTM1<sup>14</sup> which was proved to inhibit autophagic flux and benefit CRPC therapy<sup>35,36</sup>. These promoted us to examine whether ROR $\gamma$  was involved in mediating CRPC cell autophagy. Indeed, we found that both Elai significantly blocked CRPC cell autophagy *via* increasing ROR $\gamma$  mediated *SQSTM1* gene expression, which indicated that the inhibition on autophagy also played a role in ROR $\gamma$  inhibitor blocking CRPC tumor growth. It was in line with previous reports, in which Elai increased expression of SQSTM1 and acted as an autophagy inhibitor to exert anti tumor activity in ovarian cancer cells<sup>29</sup>. These data suggest that Elai, as a novel ROR $\gamma$  inhibitor, might also exert anti-tumor activity through inhibiting autophagic flux. However, the exact role of autophagy in ROR $\gamma$  inhibition suppressed CRPC tumor growth remained to be further investigated.

## 5. Conclusions

We demonstrate here that Elai is a novel ROR $\gamma$  inhibitor. It strongly inhibited CRPC cell growth *in vitro* and *in vivo* *via* suppressing ROR $\gamma$  activity and downstream programs. Our data suggest that Elai could be used as a drug candidate for the treatment of human CRPC and might be able to overcome anti-androgen therapeutic resistance.

## Acknowledgements

This research was supported by the National Natural Science Foundation of China (81872891, 81572925, 81774339 and 41776169), the Guangdong Natural Science Funds for Distinguished Young Scholar (No. 2019B151502016, China), the Science and Technology Planning Project of Guangdong Province (No. 2017A050506042, China), Local Innovative and Research Teams Project of Guangdong Pearl River Talents Program (2017BT01Y093, China), National Major Special Projects for the Creation and Manufacture of New Drugs (2019ZX09301104, China), National Engineering and Technology Research Center for New drug Druggability Evaluation (Seed Program of

Guangdong Province, 2017B090903004, China), the Fundamental Research Funds for the Central Universities (No. 19ykzd23, China), Pearl River S&T Nova Program of Guangzhou (No. 201710010136, China).

## Author contributions

Junjian Wang, Fanghai Han, Yonghong Liu, Hong-Wu Chen, Peiqing Liu and Songtao Xiang designed experiments. Jianwei Zheng, Junfeng Wang, Qian Wang, Hongye Zou, Hong Wang, Zhenhua Zhang, Jianghe Chen, Qianqian Wang and Panxia Wang carried out experiments. Jing Lu, Xiaolei Zhang, Haibin Wang and Jinping Lei analyzed experimental results. Junjian Wang, Fanghai Han, Yonghong Liu, Hong-Wu Chen, Peiqing Liu, Jianwei Zheng and Yueshan Zhao wrote the manuscript. All authors have given approval to the final version of the manuscript.

## Conflicts of interest

The authors declare no conflicts of interest.

## Appendix A. Supporting information

Supporting data to this article can be found online at <https://doi.org/10.1016/j.apsb.2020.07.001>.

## References

1. Lv G, Sun D, Zhang J, Xie X, Wu X, Fang W, et al. Lx2-32c, a novel semi-synthetic taxane, exerts antitumor activity against prostate cancer cells *in vitro* and *in vivo*. *Acta Pharm Sin B* 2017;**7**:52–8.
2. Chang AJ, Autio KA, Roachet MRd, Scher HI. High-risk prostate cancer-classification and therapy. *Nat Rev Clin Oncol* 2014;**1**:308–23.
3. Heidenreich A, Pfister D, Merseburgeret A, Bartsch G. Castration-resistant prostate cancer: where we stand in 2013 and what urologists should know. *Eur Urol* 2013;**64**:260–5.
4. Antonarakis ES, Lu C, Wang H, Lubner B, Nakazawa M, Roeser JC, et al. AR-V7 and resistance to enzalutamide and abiraterone in prostate cancer. *N Engl J Med* 2014;**371**:1028–38.
5. Augello MA, Den RB, Knudsen KE. AR function in promoting metastatic prostate cancer. *Canc Metastasis Rev* 2014;**33**:399–411.
6. Efsthioeu E, Titus M, Wenet S, Hoang A, Karlou M, Ashe R, et al. Molecular characterization of enzalutamide-treated bone metastatic castration-resistant prostate cancer. *Eur Urol* 2015;**67**:53–60.
7. Lu J, Van der Steen T, Tindall DJ. Are androgen receptor variants a substitute for the full-length receptor?. *Nat Rev Urol* 2015;**12**:137–44.
8. Kojetin DJ, Burris TP. REV-ERB and ROR nuclear receptors as drug targets. *Nat Rev Drug Discov* 2014;**13**:197–216.
9. Solt LA, Burris TP. Action of RORs and their ligands in (patho) physiology. *Trends Endocrinol Metabol* 2012;**23**:619–27.
10. Sun N, Guo H, Wang Y. Retinoic acid receptor-related orphan receptor  $\gamma$ -t (ROR $\gamma$ t) inhibitors in clinical development for the treatment of autoimmune diseases: a patent review (2016–present). *Expert Opin Ther Pat* 2019;**29**:663–74.
11. Ciofani M, Madar A, Galan C, Sellars M, Mace K, Pauli F, et al. A validated regulatory network for Th17 cell specification. *Cell* 2012;**151**:289–303.
12. Xiao S, Yosef N, Yang J, Wang Y, Zhou L, Zhu C, et al. Small-molecule ROR $\gamma$ t antagonists inhibit T helper 17 cell transcriptional network by divergent mechanisms. *Immunity* 2014;**40**:477–89.
13. Rene O, Fauber BP, Boenig Gde L, Burton B, Eidenschenk C, Everett C, et al. Minor structural change to tertiary sulfonamide RORc ligands led to opposite mechanisms of action. *ACS Med Chem Lett* 2015;**6**:276–81.

14. Wang J, Zou JX, Xue X, Cai D, Zhang Y, Duan Z, et al. ROR- $\gamma$  drives androgen receptor expression and represents a therapeutic target in castration-resistant prostate cancer. *Nat Med* 2016;**22**:488–96.
15. Lytle NK, Ferguson LP, Rajbhandari N, Gilroy K, Fox RG, Deshpande A, et al. A multiscale map of the stem cell state in pancreatic adenocarcinoma. *Cell* 2019;**177**:572–86.
16. Cai D, Wang J, Gao B, Li J, Wu F, Zou JX, et al. ROR $\gamma$  is a targetable master regulator of cholesterol biosynthesis in a cancer subtype. *Nat Commun* 2019;**10**:4621.
17. Cragg GM, Newman DJ. Natural products: a continuing source of novel drug leads. *Biochim Biophys Acta* 2013;**1830**:3670–95.
18. Zhi K, Wang J, Zhao H, Yang X. Self-assembled small molecule natural product gel for drug delivery: a breakthrough in new application of small molecule natural products. *Acta Pharm Sin B* 2020;**10**:913–27.
19. Demain AL, Vaishnav P. Natural products for cancer chemotherapy. *Microb Biotechnol* 2011;**4**:687–99.
20. Lindequist U. Marine-derived pharmaceuticals—challenges and opportunities. *Biomol Ther (Seoul)* 2016;**24**:561–71.
21. Khalifa SAM, Elias N, Farag MA, Chen L, Saeed A, Hegazy MF, et al. Marine natural products: a source of novel anticancer drugs. *Mar Drugs* 2019;**17**:49.
22. Wu C, Tan Y, Gan M, Wang Y, Guan Y, Hu Y, et al. Identification of elaiophylin derivatives from the marine-derived *Actinomycete streptomycetes* sp. 7-145 using PCR-based screening. *J Nat Prod* 2013;**76**:2153–7.
23. Wang J, Wang H, Wang LY, Cai D, Duan Z, Zhang Y, et al. Silencing the epigenetic silencer KDM4A for TRAIL and DR5 simultaneous induction and antitumor therapy. *Cell Death Differ* 2016;**23**:1886–96.
24. Lu J, Li J, Hu Y, Guo Z, Sun D, Wang P, et al. Chrysophanol protects against doxorubicin-induced cardiotoxicity by suppressing cellular PARylation. *Acta Pharm Sin B* 2019;**9**:782–93.
25. Lei J, Sheng G, Cheung PP, Wang S, Li Y, Gao X, et al. Two symmetric arginine residues play distinct roles in *Thermus thermophilus* Argonaute DNA guide strand-mediated DNA target cleavage. *Proc Natl Acad Sci U S A* 2019;**116**:845–53.
26. Lei J, Zhou Y, Xie D, Zhang Y. Mechanistic insights into a classic wonder drug— aspirin. *J Am Chem Soc* 2015;**137**:70–3.
27. Case DA, Darden TE, Cheatham III TE, Simmerling CL, Wang J, Duke RE, et al. *AMBER 12*. San Francisco: University of California; 2012. p. 79. Available from: <https://ambermd.org/>.
28. Zhang Y, Wu X, Xue X, Li C, Wang J, Wang R, et al. Discovery and characterization of XY101, a potent, selective, and orally bioavailable ROR $\gamma$  inverse agonist for treatment of castration-resistant prostate cancer. *J Med Chem* 2019;**62**:4716–30.
29. Zhao X, Fang Y, Yang Y, Qin Y, Wu P, Wang T, et al. Elaiophylin, a novel autophagy inhibitor, exerts antitumor activity as a single agent in ovarian cancer cells. *Autophagy* 2015;**11**:1849–63.
30. Lombard AP, Liu C, Armstrong CM, D'Abronzio LS, Lou W, Evans CP, et al. Wntless promotes cellular viability and resistance to enzalutamide in castration-resistant prostate cancer cells. *Am J Clin Exp Urol* 2019;**7**:203–14.
31. Chen CD, Welsbie DS, Tran C, Baek SH, Chen R, Vessella R, et al. Molecular determinants of resistance to antiandrogen therapy. *Nat Med* 2004;**10**:33–9.
32. Holzbeierlein J, Lal P, LaTulippe E, Smith A, Satagopan J, Zhang L, et al. Gene expression analysis of human prostate carcinoma during hormonal therapy identifies androgen-responsive genes and mechanisms of therapy resistance. *Am J Pathol* 2004;**164**:217–27.
33. Taylor BS, Schultz N, Hieronymus H, Gopalan A, Xiao Y, Carver BS, et al. Integrative genomic profiling of human prostate cancer. *Canc Cell* 2010;**18**:11–22.
34. Ferraldeschi R, Welti J, Luo J, Attard G, de Bono JS. Targeting the androgen receptor pathway in castration-resistant prostate cancer: progresses and prospects. *Oncogene* 2015;**34**:1745–57.
35. Nguyen HG, Yang JC, Kung HJ, Shi XB, Tilki D, Lara Jr PN, et al. Targeting autophagy overcomes enzalutamide resistance in castration-resistant prostate cancer cells and improves therapeutic response in a xenograft model. *Oncogene* 2014;**33**:4521–30.
36. Kranzbuhler B, Salemi S, Mortezaei A, Sulser T, Eberli D. Combined N-terminal androgen receptor and autophagy inhibition increases the antitumor effect in enzalutamide sensitive and enzalutamide resistant prostate cancer cells. *Prostate* 2019;**79**:206–14.